

Theory of the two-step spin conversion induced by the cooperative molecular distortions in spin-crossover compounds

Naoyuki Sasaki

Laboratory of Applied Mathematics, The Nippon Dental University, Fujimi, Chiyoda-ku, Tokyo 102, Japan

Takeshi Kambara

Department of Applied Physics and Chemistry, The University of Electro-Communications, Chofu, Tokyo 182, Japan

(Received 12 October 1988; revised manuscript received 7 April 1989)

Gütlich *et al.* [Chem. Phys. Lett. **91**, 348 (1982)] observed an "unusual" two-step high-spin \rightleftharpoons low-spin transition in the spin crossover compound $[\text{Fe}(\text{2-pic})_3]\text{Cl}_2 \cdot \text{C}_2\text{H}_5\text{OH}$. Recently, Petrouleas and Tuchagues [Chem. Phys. Lett. **137**, 21 (1987)] have shown that the other compound $\text{Fe}[\text{5NO}_2\text{-sal-N}(1,4,7,10)]$ exhibits a two-step spin conversion with a wider middle step. The mechanism of these unusual spin conversions are studied theoretically on the basis of the cooperative molecular distortion model [Kambara, J. Phys. Soc. Jpn. **49**, 1806 (1980) and Sasaki and Kambara, J. Chem. Phys. **74**, 3472 (1981)]. The couplings of the spin states of the Fe ion with a molecular distortion and a lattice strain are taken into account in the model. The spin conversion is induced by the intermolecular spin coupling mediated by the lattice vibration mode and the lattice strain. In the present model the two inequivalent sites occupied by equivalent iron complexes are assumed in a unit cell of the lattice. Molecular distortions of a pair of the two complexes occupying the two inequivalent sites couple with each other symmetrically and antisymmetrically. The origin of the two-step spin conversion (LL \rightarrow LH \rightarrow HH) comes mainly from the differences between the effects of the interpair interaction to the symmetric distortion and on the antisymmetric distortion. Various patterns of two-step spin conversions are obtained by changing the coupling strengths of the Fe ion with molecular distortion and with lattice strain and also the strength of interpair interaction. The essential features of the observed thermally induced two-step transitions and also the observed pressure effect to the transition may be reproduced by the present model.

I. INTRODUCTION

The phenomenon of the thermally and pressure-induced high-spin (HS) \rightleftharpoons low-spin (LS) transitions in some transition metal compounds has been actively investigated.¹⁻³ Recently, Köpen *et al.*⁴ observed an "unusual" spin transition anomaly in the spin crossover compound $[\text{Fe}(\text{2-pic})_3]\text{Cl}_2 \cdot \text{C}_2\text{H}_5\text{OH}$ (2-pic: 2-picolyamine) by Mössbauer spectroscopy and magnetic-susceptibility measurements. They observed a two-step spin conversion in the crossover region with transition temperatures at 120.7 and 114.0 K. Before that observation, only "one-step" spin transition, that is, continuous and discontinuous LS \rightleftharpoons HS transitions have been known. Kaji and Sorai⁵ have shown, based on the heat-capacity measurement, that there exist two phase transitions in the compound. Petrouleas and Tuchagues⁶ have found that another compound $\text{Fe}[\text{5NO}_2\text{-sal-N}(1,4,7,10)]$ shows a two-step spin conversion with a larger thermal plateau corresponding to an approximately equal population of HS and LS species.

We have so far studied the microscopic mechanism of the various types of the HS \rightleftharpoons LS transitions in ferrous and ferric spin crossover compounds and explained the origin of the one-step or usual spin conversion by using a model.⁷⁻⁹ The coupling of the *d* electrons in Fe ions with molecular distortions and a lattice strain is taken

into account in the model. The driving force of the HS \rightleftharpoons LS transition is the intermolecular spin coupling mediated by the lattice vibration modes and the lattice strain. The following results have been obtained based on the model. (i) The calculated temperature dependences based on the model reproduce all of the essential features of the observed thermally induced one-step spin conversion phenomena.⁸⁻¹⁰ (ii) The calculated pressure dependences reproduce the essential features of the observed various patterns for the pressure-induced HS \rightleftharpoons LS transitions of the ferrous and ferric compounds.¹¹⁻¹⁴ We note especially that the mechanism of the unusual pressure effect, which the model has clarified, is that the HS state with a larger volume is stabilized by pressure. (iii) The effect of a magnetic field on the HS \rightleftharpoons LS transition is considered based on the model.¹⁵ We show that the spin conversion associated with a cooperative molecular distortion is possible to control by using a magnetic field. (iv) The effect of partial substitution of the Fe ion with other transition-metal ions in spin crossover compounds is also studied based in the model.^{7,16} We clarify the mechanism of the two types of dilution effects, where the transition temperature for spin conversion decreases with decreasing Fe concentration in some spin crossover compounds but the temperature increases in another compound.

In order to make clear the mechanism of the new type

of spin conversion, that is the two-step HS \rightleftharpoons LS transition [(LS)(LS) \rightleftharpoons (LS)(HS) \rightleftharpoons (HS)(HS)], we apply the model to the case where the two inequivalent sites for iron complexes are included in a unit cell of the lattice constructed with equivalent spin crossover complexes. Molecular distortions of a pair of the two complexes occupy the inequivalent sites coupled with each other symmetrically and antisymmetrically. The intermolecular spin state coupling is mainly induced by the lattice vibration modes arising from the symmetric and antisymmetric distortions.

The origin of the two-step spin conversion comes mainly from the difference between the effect of interpair interaction on the symmetric distortion and on the antisymmetric distortion. The intramolecular coupling of the Fe ion with the molecular distortion, and the coupling with the lattice strain also affects the pattern of two-step spin conversion. The observed thermally induced two-step transitions and the observed pressure effects to the transition¹⁷ may be qualitatively reproduced by the present model.

II. DESCRIPTION OF THE MODEL

The system considered is constructed with one kind of Fe(II) complex and includes the 2N complexes. We assume that two inequivalent sites for the complexes exist in the system. These two cases of site inequivalence are considered. In one case, the complexes are distributed on two kinds (*A* and *B*) of sublattices such as the NaCl lattice structure, where any site of the *A* (*B*) sublattice is surrounded by six sites of the *B* (*A*) sublattice. In the other case, the system has a layer structure and includes two kinds (*A* and *B*) of layers which are arranged alternately. The spin crossover compounds [Fe(2-pic)₃]X₂·C₂H₅OH (*X* = Cl, Br) have a layer structure^{18,19} where the complexes in a layer are tightly bound to each other through the hydrogen bonding due to halogen ions *X*.

The Fe(II) ion in each iron molecule is surrounded by bulky ligand complexes. The ligand field has an orthorhombic or lower symmetry^{18,19} and gives rise to two possible ground states, the high-spin state ⁵Γ(*S* = 2) and the low-spin state ¹A₁(*S* = 0) in each ferrous ion, where Γ is the lowest orbital state among the three states of the *T*₂ state split by the low-symmetry ligand field. We take into account the coupling of Fe ions with the displacements of ligands with *A*_{1g} symmetry, which means a uniform dilation-contraction *Q*₁ of the iron molecule. The *A*_{1g} distortion mode *Q*₁ of each molecule is coupled with the *A*_{1g} distortion mode of other molecules through intermolecular interaction. Since the electric field for the 3*d* electrons is changed by the variation of intermolecular bond distances, we also take into account a coupling between the Fe ion and the lattice distortion with *A*_{1g} symmetry.

We consider hereafter only the system with the *AB* sublattice structure, because the final equations have similar expressions for both the sublattice and the layer systems, although the physical meanings of the expressions are slightly different between the two systems.

The Hamiltonian of the system is represented as

$$H = H_e + H_M + H_L + H_{eM} + H_{eL} . \quad (2.1)$$

The first term *H_e* is the Hamiltonian for the *d* electrons of iron ions in the undistorted system, and is given by

$$H_e = \sum_{j=1}^N \sum_{\alpha=A,B} [f_{\alpha j} + V_{0\alpha}(j)] , \quad (2.2)$$

where *f_{αj}* and *V_{0α(j)}* are the Hamiltonian for a free iron ion and the ligand field, respectively, in the *j*th molecule of the *α* sublattice (*α* = *A, B*). The second term *H_M* in (2.1),

$$H_M = \frac{1}{2} \sum_{n=1}^2 \sum_{\mathbf{k}} \frac{1}{M_n} P_n^*(\mathbf{k}) P_n(\mathbf{k}) + \frac{1}{2} \sum_{n=1}^2 \sum_{\mathbf{k}} M_n \omega_n(\mathbf{k})^2 Q_n^*(\mathbf{k}) Q_n(\mathbf{k}) , \quad (2.3)$$

is the Hamiltonian for the lattice vibration modes *Q*₁(*k*) and *Q*₂(*k*), where *Q_n*(*k*) are the normal coordinates of the modes and are written as

$$Q_n(\mathbf{k}) = \frac{1}{\sqrt{N}} \sum_{j=1}^N Q_{nj} e^{i\mathbf{k}\cdot\mathbf{R}_j} \quad (n=1,2) , \quad (2.4)$$

and *P_n*(*k*) is the canonical conjugate momentum to *Q_n*(*k*). *Q*_{1*j*} represents the symmetrical coupled distortion mode of the *j*th pair of *A* and *B* site molecules,

$$Q_{1j} = \frac{1}{\sqrt{2}} (Q_{Aj} + Q_{Bj}) , \quad (2.5)$$

and *Q*_{2*j*} represents the antisymmetrically coupled mode,

$$Q_{2j} = \frac{1}{\sqrt{2}} (Q_{Aj} - Q_{Bj}) , \quad (2.6)$$

where *Q_{αj}* represents the *A*_{1g} displacement of ligands around the Fe ion in the *α* site molecule of the *j*th pair. The third term *H_L* in (2.1),

$$H_L = NC_1 U_1^2 , \quad (2.7)$$

is the elastic energy of the lattice strain *U*₁ with *A*_{1g} symmetry, where

$$C_1 = 3B\Omega_0 , \quad (2.8)$$

B is the bulk modulus, and *Ω*₀ is the volume per Fe ion. The fourth term *H_{eM}*, in (2.1),

$$H_{eM} = \sum_{j=1}^N (X_{Aj} Q_{Aj} + X_{Bj} Q_{Bj}) , \quad (2.9)$$

represents the interaction between the *d* electrons and the molecular displacements *Q_{αj}*. The electronic operators *X_{αj}* are given by

$$X_{\alpha j} = [\partial V_{\alpha}(j) / \partial Q_{\alpha j}]_0 \quad (\alpha = A, B) , \quad (2.10)$$

where *V_{α(j)}* is the ligand field for the Fe ion of *α* site molecule of the *j*th pair. The final term *H_{eL}* in (2.1),

$$H_{eL} = \sum_{j=1}^N (Y_{Aj} U_1 + Y_{Bj} U_1) , \quad (2.11)$$

is the interaction between the d electrons and the lattice strain U_1 . The electronic operators $Y_{\alpha j}$ are given by

$$Y_{\alpha j} = [\partial V_{\alpha}(j)/\partial U_1]_0 \quad (\alpha = A, B). \quad (2.12)$$

In order to obtain the eigenvalues and eigenfunctions of H , we eliminate the interactions H_{eM} by a canonical transformation

$$\hat{P}_n(\mathbf{k}) = P_n(\mathbf{k}), \quad (2.13)$$

$$\hat{Q}_n(\mathbf{k}) = Q_n(\mathbf{k}) + \frac{X_n(\mathbf{k})}{M_n \omega_n(\mathbf{k})^2} \quad (n = 1, 2), \quad (2.14)$$

where

$$X_n(\mathbf{k}) = \frac{1}{\sqrt{N}} \sum_{j=1}^N \frac{1}{\sqrt{2}} (X_{Aj} \pm X_{Bj}) e^{i\mathbf{k} \cdot \mathbf{R}_j} \quad (2.15)$$

(use $+$ for $n=1$ and $-$ for $n=2$). The Hamiltonian H then is represented as

$$H = H_e + H_{ee} + \hat{H}_M + H_L + H_{eL}, \quad (2.16)$$

where

$$\begin{aligned} \hat{H}_M = & \frac{1}{2} \sum_{n=1}^2 \sum_{\mathbf{k}} \frac{1}{M_n} \hat{P}_n^*(\mathbf{k}) \hat{P}_n(\mathbf{k}) \\ & + \frac{1}{2} \sum_{n=1}^2 \sum_{\mathbf{k}} M_n \omega_n(\mathbf{k})^2 \hat{Q}_n^*(\mathbf{k}) \hat{Q}_n(\mathbf{k}), \end{aligned} \quad (2.17)$$

$$\begin{aligned} h_j = & \sum_{\alpha=A,B} [f_{\alpha j} + V_{\alpha}(j)] + C_1 U_1^2 + \frac{1}{2} K_1 (\langle X_A \rangle^2 + \langle X_B \rangle^2) + K_2 \langle X_A \rangle \langle X_B \rangle \\ & - \frac{1}{2} K_0 (X_{Aj}^2 + X_{Bj}^2) - (K_1 \langle X_A \rangle + K_2 \langle X_B \rangle) X_{Aj} - (K_2 \langle X_A \rangle + K_1 \langle X_B \rangle) X_{Bj} + U_1 Y_{Aj} + U_1 Y_{Bj}, \end{aligned} \quad (2.22)$$

where

$$K_0 = \frac{1}{2N} \sum_{\mathbf{k}} \sum_{n=1}^2 \frac{1}{M_n \omega_n(\mathbf{k})^2}, \quad (2.23)$$

$$K_1 = \frac{1}{2} \sum_{n=1}^2 \frac{1}{M_n \omega_n(0)^2} - K_0, \quad (2.24)$$

$$K_2 = \frac{1}{2M_1 \omega_1(0)^2} - \frac{1}{2M_2 \omega_2(0)^2}. \quad (2.25)$$

We consider the physical meanings of the terms including X_{α} in (2.22). It is seen from the analogy with the spin Hamiltonian for antiferromagnetic systems that $\langle X_{\alpha} \rangle$ represents a kind of molecular field at the α site. Since the thermal equilibrium value of the transformed coordinate $\langle \hat{Q}_n(\mathbf{k}) \rangle$, is zero, that of the real displacement $Q_n(\mathbf{k})$ is obtained from (2.14) as

$$\langle Q_n(\mathbf{k}) \rangle = - \frac{\langle X_n(\mathbf{k}) \rangle}{M_n \omega_n(\mathbf{k})^2}. \quad (2.26)$$

Using (2.4)–(2.6) and (2.15), we obtain

$$\begin{aligned} H_{ee} = & -\frac{1}{4} \sum_{j,l} J_{jl} (X_{Aj} + X_{Bj})(X_{Al} + X_{Bl}) \\ & -\frac{1}{4} \sum_{j,l} K_{jl} (X_{Aj} - X_{Bj})(X_{Al} - X_{Bl}). \end{aligned} \quad (2.18)$$

Here the electronic coupling strengths J and K between the j th and l th pairs are given by

$$J_{jl} = \frac{1}{N} \sum_{\mathbf{k}(\neq 0)} \frac{1}{M_1 \omega_1(\mathbf{k})^2} e^{-i\mathbf{k} \cdot (\mathbf{R}_j - \mathbf{R}_l)}, \quad (2.19)$$

$$K_{jl} = \frac{1}{N} \sum_{\mathbf{k}(\neq 0)} \frac{1}{M_2 \omega_2(\mathbf{k})^2} e^{-i\mathbf{k} \cdot (\mathbf{R}_j - \mathbf{R}_l)}. \quad (2.20)$$

We adopt the random-phase approximation to make the calculation feasible. The operators $X_{\alpha j} X_{\beta l}$ with $(\alpha j \neq \beta l)$ in H_{ee} are replaced by

$$\begin{aligned} X_{\alpha j} X_{\beta l} = & X_{\alpha j} \langle X_{\beta l} \rangle + X_{\beta l} \langle X_{\alpha j} \rangle \\ & - \langle X_{\alpha j} \rangle \langle X_{\beta l} \rangle \quad (\alpha, \beta = A \text{ or } B), \end{aligned} \quad (2.21)$$

where $\langle X_{\alpha j} \rangle$ represents the thermal average of the operator $X_{\alpha j}$ and does not depend on the suffix j , because the average value of $X_{\alpha j}$ is equal for every α site molecule, and it is written as $\langle X_{\alpha} \rangle$. Substituting (2.21) into (2.18), and using the fact that H_{ee} has the total (A_{1g}) symmetry, the final form of the electronic Hamiltonian is written as the sum of the Hamiltonian h_j for single pair of A and B site molecules,

$$\begin{aligned} \langle X_{\alpha} \rangle = & -\frac{1}{\sqrt{2}} [M_1 \omega_1(0)^2 + M_2 \omega_2(0)^2] \langle Q_{\alpha} \rangle \\ & - \frac{1}{\sqrt{2}} [M_1 \omega_1(0)^2 - M_2 \omega_2(0)^2] \langle Q_{\beta} \rangle, \end{aligned} \quad (2.27)$$

where $(\alpha, \beta) = (A, B)$ or (B, A) . The molecular field $\langle X_{\alpha} \rangle$ is given by the linear combination of the cooperative intramolecular distortions $\langle Q_A \rangle$ and $\langle Q_B \rangle$. Therefore, $X_{\alpha j}$ may be interpreted as an operator describing the molecular distortion of the j th molecule at the α site. Thus, we may interpret each term including X_{α} in (2.22) as follows: The third term

$$[K_1 (\langle X_A \rangle^2 + \langle X_B \rangle^2) / 2]$$

corresponds to the elastic energy for the cooperative molecular distortions. The fourth term indicates a coupling between them, which occurs only when the force constant $M_n \omega_n(0)^2$ differs between the symmetrically and the antisymmetrically coupled pair distortions, as seen from (2.25). The fifth term

$$K_0 (X_{Aj}^2 + X_{Bj}^2) / 2$$

corresponds to the energy gain due to the individual distortion of each molecule which does not vanish even at

temperatures so high that the cooperative distortions $\langle X_\alpha \rangle$ disappear. The sixth and seventh terms correspond to the energy gain or loss due to the individual molecular distortion in the molecular fields $\langle X_A \rangle$ and $\langle X_B \rangle$, where the intersublattice interaction terms $\langle X_B \rangle X_{Aj}$ and $\langle X_A \rangle X_{Bj}$ occur only in the case of

$$M_1 \omega_1(\mathbf{0})^2 \neq M_2 \omega_2(\mathbf{0})^2.$$

If there is no intermolecular interaction, K_1 in (2.24) is zero because $\omega_n(\mathbf{k}) \equiv \omega_n(\mathbf{0})$ for any \mathbf{k} . That is, the intrasublattice interaction terms $\langle X_\alpha \rangle X_{\alpha j}$ arise from the intermolecular interaction within the α sublattice.

$$E_1 = E_0 - w_0 a^2 + (1 + w_2) a q_A + (1 + w_2) a q_B + 2b u_1, \quad (2.28)$$

$$E_2 = \varepsilon_0 + E_0 - \frac{1}{2} w_0 (1 + \lambda^2) a^2 + (1 + \lambda w_2) a q_A + (\lambda + w_2) a q_B + b(1 + \mu) u_1, \quad (2.29)$$

$$E_3 = \varepsilon_0 + E_0 - \frac{1}{2} w_0 (1 + \lambda^2) a^2 + (\lambda + w_2) a q_A + (1 + \lambda w_2) a q_B + b(1 + \mu) u_1, \quad (2.30)$$

$$E = 2\varepsilon_0 + E_0 - w_0 \lambda^2 a^2 + (1 + w_2) \lambda a q_A + (1 + w_2) \lambda a q_B + 2\mu b u_1, \quad (2.31)$$

where

$$E_0 = \frac{1}{2} u_1^2 + \frac{1}{2} (q_A^2 + q_B^2) + w_2 q_A q_B, \quad (2.32)$$

$$\varepsilon_0 = \langle \psi_{\alpha H} | f_{\alpha j} + V_{0\alpha}(j) | \psi_{\alpha H} \rangle - \langle \psi_{\alpha L} | f_{\alpha j} + V_{0\alpha}(j) | \psi_{\alpha L} \rangle, \quad (2.33)$$

$$q_A = -(K_1)^{1/2} \langle X_A \rangle, \quad (2.34)$$

$$q_B = -(K_1)^{1/2} \langle X_B \rangle, \quad (2.35)$$

$$u_1 = (C_1)^{1/2} U_1, \quad (2.36)$$

$$a = (K_1)^{1/2} \langle \psi_{\alpha L} | X_{\alpha j} | \psi_{\alpha L} \rangle \quad (\alpha = A, B), \quad (2.37)$$

$$\lambda a = (K_1)^{1/2} \langle \psi_{\alpha H} | X_{\alpha j} | \psi_{\alpha H} \rangle, \quad (2.38)$$

$$b = \langle \psi_{\alpha L} | Y_{\alpha j} | \psi_{\alpha L} \rangle / (C_1)^{1/2}, \quad (2.39)$$

$$\mu b = \langle \psi_{\alpha H} | Y_{\alpha j} | \psi_{\alpha H} \rangle / (C_1)^{1/2}, \quad (2.40)$$

$$w_0 = \frac{K_0}{K_1}, \quad w_2 = \frac{K_2}{K_1}. \quad (2.41)$$

Since q_A and q_B are interpreted as quantities representing the cooperative intramolecular distortions in the A and B sublattices, respectively, it is seen in (2.28)–(2.31) that the eigenvalues are determined by the cooperative intramolecular distortions and the lattice strain u_1 through the relevant coupling strengths, a , λa , b , and μb .

III. BASIC EQUATIONS IN THE THERMODYNAMIC EQUILIBRIUM

The thermodynamic equilibrium state of the system at constant pressure is found by minimizing the free energy G with respect to q_A and q_B subject to the condition that the values of q_α should satisfy (2.34) and (2.35) self-consistently. The free energy at constant pressure is

The eigenvalues and eigenfunctions of h_j are calculated within the four electronic states whose wave functions are represented as $\Psi_1 = \psi_{AL} \psi_{BL}$, $\Psi_2 = \psi_{AL} \psi_{BH}$, $\Psi_3 = \psi_{AH} \psi_{BL}$ and

$$\Psi_4 = \psi_{AH} \psi_{BH},$$

where $\psi_{\alpha L} = |^1A_1\rangle$ is the wave function of the low-spin 1A_1 state of Fe(II) ion in the α molecule, and $\psi_{\alpha H} = |^5\Gamma M_S\rangle$ is that of high-spin $^5\Gamma$ state with spin z component of M_S . The eigenvalues for Ψ_n ($n=1-4$) are written as

given by

$$G = -k_B T \ln Y(T, P), \quad (3.1)$$

$$Y(T, P) = \int_0^\infty Z(T, \Omega) e^{-P\Omega/k_B T} d\Omega, \quad (3.2)$$

$$Z(T, \Omega) = \left[\sum_{n=1}^4 g_n e^{-E_n/k_B T} \right]^N, \quad (3.3)$$

where P and Ω denote the pressure and volume of the system, respectively, and g_n is the degeneracy of the n th state Ψ_n , $g_1 = 1$, $g_2 = 5$, $g_3 = 5$, and $g_4 = 25$.

We approximate the integration in (3.2) by using the maximum value of the integrand and obtain

$$Y(T, P) = Z(T, \Omega^*) e^{-P\Omega^*/k_B T} \Delta\Omega, \quad (3.4)$$

where the most probable volume Ω^* is determined by

$$P = k_B T \partial \ln Z(T, \Omega^*) / \partial \Omega^*. \quad (3.5)$$

The volume Ω is assumed to stay in the region around Ω^* and is then given by

$$\Omega = N\Omega_0 (1 + (3/C_1)^{1/2} u_1), \quad (3.6)$$

where Ω_0 is the volume in case of no lattice strain. Then the equilibrium values of the cooperative intramolecular distortions q_A and q_B are obtained from $\partial G / \partial q_A = 0$ and $\partial G / \partial q_B = 0$. The results are represented as

$$q_A = -a(\rho_1 + \rho_2) - \lambda a(\rho_3 + \rho_4), \quad (3.7)$$

$$q_B = -a(\rho_1 + \rho_3) - \lambda a(\rho_2 + \rho_4), \quad (3.8)$$

where ρ_n is the population of the n th level and is given by

$$\rho_n = g_n \exp(-E_n/k_B T) / \sum_{m=1}^4 g_m \exp(-E_m/k_B T). \quad (3.9)$$

By substituting (3.3) into (3.5) and using (3.6), we obtain the equilibrium lattice strain u_1 under the pressure P . It is represented as

$$u_1 = -(3/C_1)^{1/2} P \Omega_0 - b [2\rho_1 + (1+\mu)(\rho_2 + \rho_3) + 2\mu\rho_4]. \quad (3.10)$$

If the values of the internal parameters ε_0 , a , b , λ , μ , w_0 , and w_2 and of the external parameters T and P are given, we obtain the values of the cooperative intramolecular distortions, q_A , q_B , and the lattice strain u_1 by using (3.7), (3.8), and (3.10).

The dependences of the high-spin fraction ρ_H on temperature T and pressure P are calculated by

$$\rho_H = \frac{1}{2}\rho_2 + \frac{1}{2}\rho_3 + \rho_4. \quad (3.11)$$

We obtain a linear relation between ρ_H and u_1 from (3.10) and (3.11) as

$$u_1 = 2b(1-\mu)\rho_H - (3/C_1)^{1/2} P \Omega_0 - 2b. \quad (3.12)$$

IV. CALCULATED RESULTS FOR THE SPIN STATE TRANSITIONS

A. The values of relevant parameters

In order to further the calculation, we need the values for the internal parameters ε_0 , a , b , λ , μ , w_0 , and w_2 as well as the external parameter $P\Omega_0(C_1)^{1/2}$. The values for the energy separation ε_0 between the 1A_1 and $^5\Gamma$ states are of the order of 1000 cm^{-1} for many iron complexes.²⁰ The values of b , μ , and $P\Omega_0/(C_1)^{1/2}$ have been estimated in previous papers,^{7,11,12} and the reasonable results for temperature and pressure dependences of one-step HS \rightleftharpoons LS transitions have been obtained by using those values. The coupling parameters b (2.39) and μb (2.40) between an Fe ion and the lattice strain in the low-spin state and in the high-spin state, respectively, have been estimated^{7,11} such that the value of b is in the region of -10 – $10 \text{ cm}^{-1/2}$ and μ takes a value in the range from 1 to 3 for $b < 0$ and from -1 to 1 for $b > 0$, respectively. We have had no reasonable estimation yet for the intramolecular coupling parameters a (2.37) and λa (2.38) between the d electrons and the intramolecular dilation Q_α in the low-spin state and in the high-spin state, respectively. In order to estimate the magnitudes of a and λa , we evaluate them for an octahedral Fe(II) L_6^- cluster in the point charge approximation.⁷ The results are

$$a/(K_1)^{1/2} = -1.5 \times 10^5 \text{ cm}^{-1}/R_0$$

and

$$\lambda a/(K_1)^{1/2} = -3.1 \times 10^5 \text{ cm}^{-1}/R_0,$$

where R_0 is the length of bond (Fe—L). Then λ is near to 2. The shift of the bond length (Fe—L) induced by the HS \rightleftharpoons LS is estimated by $\langle Q_\alpha \rangle_{\text{HS}} - \langle Q_\alpha \rangle_{\text{LS}}$, where

$\langle Q_\alpha \rangle_{\text{HS}}$ and $\langle Q_\alpha \rangle_{\text{LS}}$ correspond to the thermally averaged shifts of bond length in the complete high-spin and low-spin states, respectively. It is seen from (2.27) and (2.34) that

$$\langle Q_\alpha \rangle \approx \langle q_\alpha \rangle / [(2K_1)^{1/2} M \omega(\mathbf{0})^2].$$

The values of $\langle q_\alpha \rangle$ in the complete low-spin and high-spin states are obtained from $\partial E_1 / \partial q_\alpha = 0$ and $\partial E_4 / \partial q_\alpha = 0$, respectively, and are $\langle q_\alpha \rangle_{\text{LS}} \approx -a$ and $\langle q_\alpha \rangle_{\text{HS}} \approx -\lambda a$. Thus, the bond shift ΔR is approximated as

$$\Delta R \approx (1-\lambda)[a/(K_1)^{1/2}] / [\sqrt{2} M \omega(\mathbf{0})^2].$$

When we take $\Delta R = 0.2 \text{ \AA}$ and $R_0 = 2 \text{ \AA}$ as observed for $[\text{Fe}(\text{phen})_2(\text{NCS})_2]^{21}$, $M \omega(\mathbf{0})^2$ becomes of the order of 10^5 g/s^2 . Since the values of K_1 are estimated to be around $1/[5M \omega(\mathbf{0})^2]$ from the consideration mentioned below, a and λa become of the order of $10 \text{ cm}^{-1/2}$. Furthermore, we have estimated^{8,10} the values of the coupling parameter (λa) for the intramolecular distortion with E_g symmetry. The values are of the order of $10 \text{ cm}^{-1/2}$. Therefore, we estimate that the value of a is in the region of -50 – $0 \text{ cm}^{-1/2}$, and the ratio λ takes a value around 2.

We now consider the values of w_0 and w_2 as defined in (2.41). First, we estimate the reciprocal force constants of the lattice vibration modes, K_0 (2.23), K_1 (2.24), and K_2 (2.25). K_0 is the reciprocal force constant averaged over the symmetric and antisymmetric modes and over all the \mathbf{k} space, it is always positive. K_1 is the difference between the reciprocal force constants of the Γ point ($\mathbf{k}=\mathbf{0}$) and the value averaged over all the \mathbf{k} space. When the dispersion curve $\omega_n(\mathbf{k})$ is concave (convex) around the Γ point, K_1 may become positive (negative). Since the frequency dispersion $|\omega_n(\mathbf{k}) - \omega_n(\mathbf{0})|$, of the lattice vibration mode increases as the strength of intermolecular interaction increases, K_1 becomes larger with the intermolecular interaction. We assume that the width of the dispersion,

$$|\omega_n(\mathbf{k}_{\text{max}}) - \omega_n(\mathbf{0})|,$$

ranges from $\omega_n(\mathbf{0})/10$ to $\omega_n(\mathbf{0})$. Then, as is seen in (2.24), the values of K_1 range from $1/[10M \omega(\mathbf{0})^2]$ to $1/[M \omega(\mathbf{0})^2]$. Since the values of K_0 are of the order of $1/[M \omega(\mathbf{0})^2]$, the values of $|w_0| = K_0/|K_1|$ range from 1 to 10. K_2 is the difference between the reciprocal force constants for the symmetric mode and those for the antisymmetric mode at Γ point. We assume that the difference between $M_1 \omega_1(\mathbf{0})^2$ and $M_2 \omega_2(\mathbf{0})^2$ is at largest $M_n \omega_n(\mathbf{0})^2/10$. Then it is seen from (2.25) that K_2 is less than $1/[10M_n \omega_n(\mathbf{0})^2]$. Since $|w_2| = |K_2/K_1|$ is less than 1, we take a value between -1 and 1 for w_2 .

The external parameters are temperature T and pressure P . We change the value of T from 0 to 400 K. Since the pressure is included in a form of $(3/C_1)^{1/2} P \Omega_0$ in (3.10), we define a new parameter as

$$p = (3/C_1)^{1/2} P \Omega_0. \quad (4.1)$$

The value of p is changed from 0 to $330 \text{ cm}^{-1/2}$, where the range corresponds to that of P from 0 to 200 kbar.¹¹

B. Temperature dependences of the cooperative molecular distortions q_A and q_B and of the high-spin fraction ρ_H for $P=0$

We study how the pattern of temperature dependences of q_A , q_B , and ρ_H change with the values of the coupling parameters especially giving attention to the condition for the appearance of the two-step spin conversion: The temperature dependences of the equilibrium cooperative molecular distortions q_A and q_B with A_{1g} symmetry, the lattice strain u_1 and the high-spin fraction ρ_H are calculated as functions of the energy difference ϵ_0 and the coupling parameters a , b , w_0 , and w_2 . The equilibrium values of q_A , q_B , and u_1 are obtained from (3.7), (3.8), and (3.10), respectively.

In this subsection we consider only the case of $P=0$. The temperature dependences of q_A and q_B are shown in Fig. 1 as a function of the difference w_2 between the reciprocal reduced force constants of the symmetric and antisymmetric vibration modes, where $\epsilon_0=2950 \text{ cm}^{-1}$, $a=-18 \text{ cm}^{-1/2}$, $b=-4 \text{ cm}^{-1/2}$, $w_0=5.0$, $\lambda=2$, and $\mu=2.0$. When w_2 is positive, no discontinuous transition appears, and the A and B site molecules contract symmetrically. On the other hand, when w_2 is negative and the strength is not so strong ($-0.3 \leq w_2 < 0$), the discontinuous transition occurs at the two definite temperatures, T_{c1} and T_{c2} . At lower temperature $T < T_{c1}$, the cooperative molecular distortions of A and B site molecules are equal ($q_A=q_B$) and increase with temperature. At the first transition temperature T_{c1} , the molecular distortion of one of the two sites molecules, q_A , increases abruptly while that of the other site molecule, q_B , slightly decreases. In the temperature range of $T_{c1} < T < T_{c2}$, q_A decreases and q_B increases gradually with increasing temperature; that is, q_A and q_B change antisymmetrically.

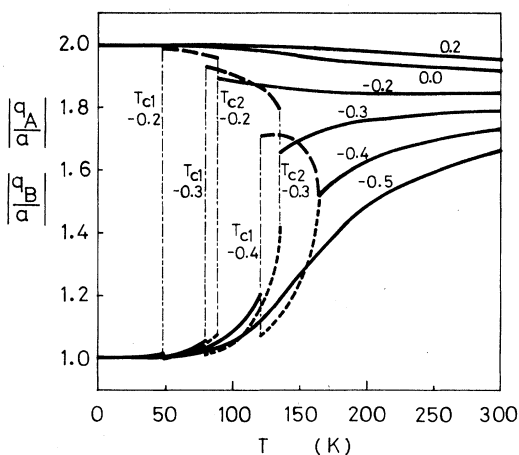


FIG. 1. The calculated temperature dependence of the cooperative molecular distortions q_A and q_B as functions of w_2 , where $\epsilon_0=2950 \text{ cm}^{-1}$, $a=-18 \text{ cm}^{-1/2}$, $b=-4 \text{ cm}^{-1/2}$, $w_0=5.0$, $\lambda=2.0$, and $\mu=2.0$. The dot-dashed and dashed curves represent $|q_A/a|$ and $|q_B/a|$, respectively, and the solid curve denotes $|q_A/a|$ and $|q_B/a|$ in the case of $|q_A|=|q_B|$. The figures at the side of the transition lines (dot-dashed lines) denote the values of w_2 .

At the second transition temperature T_{c2} , the abrupt change in the molecular distortions occurs again and for $T > T_{c2}$, q_A becomes equal to q_B once more; that is, A and B site molecules distort symmetrically. In the case of $-0.5 < w_2 \leq -0.4$, the first transition at T_{c1} is discontinuous, but the second transition becomes continuous. When w_2 is negative and w_2 is large enough, there is no two-step transition and the continuous low-spin \leftrightarrow high-spin transitions occur.

The temperature dependence of the lattice strain u_1 is shown in Fig. 2 as a function of w_2 in the case where the values of ϵ_0 , a , b , w_0 , λ , and μ are the same as in Fig. 1. The discontinuous transitions of u_1 occur at the same temperatures for q_A and q_B . The dependence of transition pattern of u_1 on w_2 is equivalent to those of q_A and q_B . The temperature dependences of the high-spin fraction ρ_H are obtained from the temperature dependences of u_1 by using (3.12). The results are shown as a function of w_2 in Fig. 2, where the parameter values are the same as those in Fig. 1. The two-step spin state transition consisting of two discontinuous transitions, from the low-spin to the medium-spin states at T_{c1} and from the medium-spin to the high-spin states at T_{c2} , occurs for the values of w_2 , which are negative but not very small, where $-0.3 \leq w_2 < 0$ in the case of Fig. 2. The medium-spin state means the state in which the A site molecules are in the high-spin state and the B site molecules are in the low-spin state.

The two-step spin state transitions occur according to the following procedures. At very low temperature all of the molecules occupy the low-spin state with a smaller volume and with energy which is lower than that of the high-spin state. As temperature increases, some molecules occupy the high-spin state with larger volume and with degeneracy that is larger than that of the low-spin state. Then the cooperative molecular distortions q_A and q_B , which are induced by the lattice vibration modes Q_1 and Q_2 increase gradually as seen in Fig. 1. At T_{c1} the contribution of the antisymmetric mode Q_2 becomes dominant. Then all A site molecules dilate and are in the

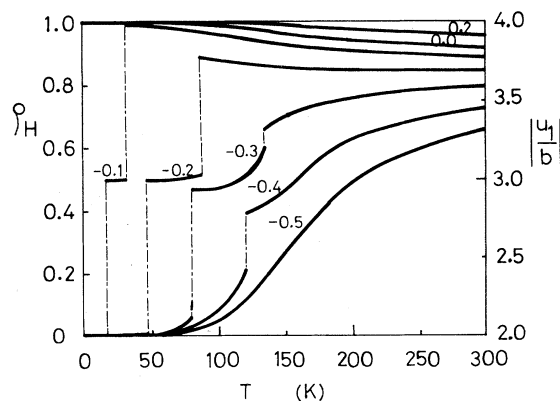


FIG. 2. The calculated temperature dependences of the high-spin fraction ρ_H and the lattice strain u_1 as functions of w_2 , where the values of ϵ_0 , a , b , w_0 , λ , and μ are the same as in Fig. 1. [u_1 is represented by ρ_H through the relation (3.12)]. The number on each curve denotes the values of w_2 .

high-spin state, and all B site molecules contract and are in the low-spin state as seen in Fig. 2. Although the contributions of the symmetric mode Q_1 and the elastic strain u_1 increase with increasing temperature, the nearly equal population of the high- and low-spin states is maintained due to the strong contribution of the Q_2 mode. However, at T_{c2} the contributions of Q_1 and u_1 overcome that of Q_2 and the difference between the cooperative distortions q_A and q_B vanishes as seen in Fig. 1. Then all of the molecules are in the high-spin state as seen in Fig. 2.

We will now consider the dependence of spin state transition on the intramolecular coupling strength a between the Fe ion and molecular distortion. The thermal variations of high-spin fraction ρ_H are shown as a function of a in Fig. 3 for $\epsilon_0=2950 \text{ cm}^{-1}$, $b=-4 \text{ cm}^{-1/2}$, $w_0=5.0$, $w_2=-0.2$, $\lambda=2.0$, and $\mu=2.0$. For the strong coupling, $|a| \geq 18.3 \text{ cm}^{-1/2}$, the system stays in the high-spin state. The two-step spin conversion becomes possible for the values of a within a very small range

$$17.8 \text{ cm}^{-1/2} \leq |a| < 18.2 \text{ cm}^{-1/2}.$$

For the weaker coupling

$$|a| \leq 17.7 \text{ cm}^{-1/2},$$

the system shows a continuous transition from low-spin to high-spin states. When ϵ_0 decreases, the values of a inducing the two-step spin conversion also decrease. For $\epsilon_0=1500 \text{ cm}^{-1}$ the values are in the region of

$$-12.9 - -12.6 \text{ cm}^{-1/2}.$$

The temperature dependence of ρ_H is calculated as a function of the energy separation ϵ_0 between the low-spin and the high-spin states in the isolated molecule. In the case where the other parameter values are fixed, only the high-spin state exists in the system for smaller values of ϵ_0 . For larger values of ϵ_0 only the continuous low-spin \rightleftharpoons high-spin transition occurs. The two-step spin conversion may take place for values of ϵ_0 within a rather

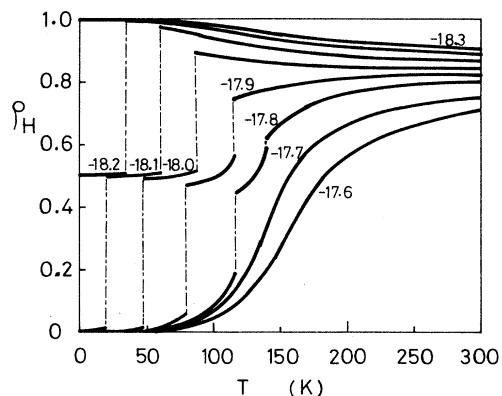


FIG. 3. The calculated temperature dependences of ρ_H as a function of the intramolecular coupling strength a between the Fe ion and molecular distortion. The parameter values are $\epsilon_0=2950 \text{ cm}^{-1}$, $b=-4 \text{ cm}^{-1/2}$, $w_0=5.0$, $w_2=-0.2$, $\lambda=2.0$, and $\mu=2.0$. The numbers on the curves denote the values of a in units of $(\text{cm}^{-1})^{1/2}$.

narrow range. Then, the transition temperatures T_{c1} and T_{c2} increase with increasing ϵ_0 . Since the effect of w_0 is taken into account by replacing ϵ_0 with

$$\epsilon_0 - \frac{1}{2}w_0(\lambda^2 - 1)a^2$$

in (2.28)–(2.31), the effect of increasing w_0 is equivalent to that of decreasing ϵ_0 .

Finally, we consider the effects of the coupling parameter b between an Fe ion and the lattice strain on the two-step spin conversion system. In the cases of $b > 0$ the low-spin state is stabilized by the lattice strain u_1 , but the state is destabilized by u_1 in the case of $b < 0$. The two-step spin conversion may occur for values of b in a comparatively wide range. For example, the range is

$$-6.5 \text{ cm}^{-1/2} < b < 2 \text{ cm}^{-1/2}$$

in the case where $\epsilon_0=2950 \text{ cm}^{-1}$, $a=-18 \text{ cm}^{-1/2}$, $w_0=5.0$, $w_2=-0.2$, $\lambda=2.0$, $\mu=2.0$ for $b < 0$ and $\mu=0.5$ for $b > 0$.

The thermally induced two-step spin conversion seems to occur only for special iron complexes, because the spin conversion becomes possible for rather narrow regions of values of the intramolecular parameters ϵ_0 and a . When the above intramolecular conditions are satisfied, the two-step spin conversion is driven by w_2 which arises from the difference between the frequency $\omega_1(0)$ of the symmetrical molecular distortion mode and that $\omega_2(0)$ of the antisymmetrical distortion mode.

C. Dependences of q_A , q_B , and ρ_H on pressure

We now consider how the patterns of spin conversion may be changed by pressure. Since the bond length between Fe and ligand ions is much shorter in the 1A_1 state than in the 5T_2 state, the low-spin state is usually stabilized by pressure. We show the pressure dependence of the high-spin fraction ρ_H at six temperatures 25, 50, 75, 100, 125, and 150 K in Fig. 4, where the values of param-

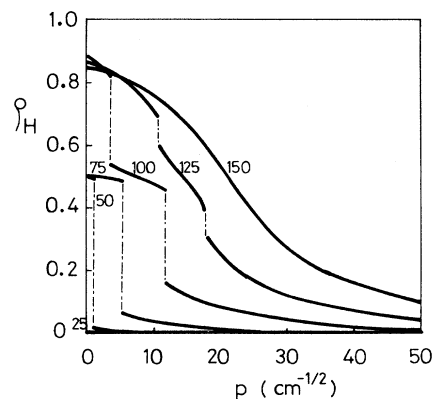


FIG. 4. The calculated pressure dependence of ρ_H as a function of temperature T . The parameter values used are $\epsilon_0=2950 \text{ cm}^{-1}$, $a=-18 \text{ cm}^{-1/2}$, $b=-4.0 \text{ cm}^{-1/2}$, $w_0=5.0$, $w_2=-0.2$, $\lambda=2.0$, and $\mu=2.0$. The numbers on the curves denote the values of T in K.

eters are $\epsilon_0=2950 \text{ cm}^{-1}$, $a=-18 \text{ cm}^{-1/2}$, $b=-4 \text{ cm}^{-1/2}$, $w_0=5.0$, $w_2=-0.2$, $\lambda=2.0$, and $\mu=2.0$. The thermally induced two-step spin conversion occurs without pressure in the case of these parameter values, where $T_{c1}=48 \text{ K}$ and $T_{c2}=90 \text{ K}$.

For the temperature range of $90 \text{ K} < T < 135 \text{ K}$ the system is in the high-spin state at zero pressure. When the pressure is increased, the system changes the spin state discontinuously from the high-spin to the medium-spin states at a definite pressure p_{c1} . With a further increase of pressure the spin state changes discontinuously from the medium-spin to the low-spin states at p_{c2} . This is the pressure induced two-step spin conversion.

It is seen by substituting the strain u_1 of (3.10) into the eigenenergies E_n of (2.28)–(2.31) that the effect of pressure is represented by the replacement of ϵ_0 with $\epsilon_0 - b(\mu - 1)p$ in the energy separation between the low- and the high-spin states. Therefore we may adjust effectively the value of the energy separation ϵ_0 in the isolated molecule by changing the pressure so that the two-step spin conversion is induced thermally. The transition temperatures T_{c1} and T_{c2} increase with increasing pressure, because the low-spin state is stabilized by pressure.

V. CONCLUDING REMARKS

We compare the qualitative features of the two-step spin conversion derived in the basis of the present model with the observed results for $[\text{Fe}(\text{2-pic})_3]\text{Cl}_2 \cdot \text{C}_2\text{H}_5\text{OH}^4$ and $\text{Fe}[\text{5NO}_2\text{-sal-N}(1,4,7,10)]$.⁶ The observed temperature dependence of the high-spin fraction ρ_H for the former compound is qualitatively equivalent to the calculated dependence for $a = -17.8 \text{ cm}^{-1/2}$ in Fig. 3. The qualitative feature of ρ_H observed for the latter compound is quite similar to the calculated result for $a = -18 \text{ cm}^{-1/2}$ in Fig. 3.

The pressure effect on the temperature dependence of ρ_H has been observed¹⁷ for $[\text{Fe}(\text{2-pic})_3]\text{Cl}_2 \cdot \text{C}_2\text{H}_5\text{OH}$. It has been shown that the transition temperatures T_{c1} and T_{c2} are shifted toward high temperature by pressure. This is also the case in the present model.

Thus, the present model may reproduce qualitatively the essential features of the observed two-step spin conversions. However, before we make a detailed quantitative comparison of the model with the experimental results, we require detailed knowledge about the values of the various parameters for the compounds in which the two-step spin conversion occurs.

¹P. Gülich, *Struct. Bonding (Berlin)* **44**, 83 (1981).

²E. König, G. Ritter, and S. K. Kulshreshtha, *Chem. Rev.* **85**, 219 (1985).

³C. N. Rao, *Int. Rev. Phys. Chem.* **4**, 19 (1985).

⁴E. Köppen, E. W. Müller, C. P. Kohler, H. P. Spiering, M. Meissner, and P. Gülich, *Chem. Phys. Lett.* **91**, 348 (1982).

⁵K. Kaji and M. Sorai, *Thermochim. Acta* **88**, 185 (1985).

⁶V. Petrouleas and J.-P. Tuchagues, *Chem. Phys. Lett.* **137**, 21 (1987).

⁷T. Kambara, *J. Phys. Soc. Jpn.* **49**, 1806 (1980).

⁸T. Kambara, *J. Chem. Phys.* **74**, 4557 (1981).

⁹N. Sasaki and T. Kambara, *J. Chem. Phys.* **74**, 3472 (1981).

¹⁰T. Kambara, *J. Chem. Phys.* **70**, 4199 (1979).

¹¹T. Kambara, *J. Phys. Soc. Jpn.* **50**, 2257 (1981).

¹²N. Sasaki and T. Kambara, *J. Phys. Soc. Jpn.* **51**, 1571 (1982).

¹³F. Ogata, T. Kambara, K. I. Gondaira, and N. Sasaki, *J. Magn. Magn. Mater.* **31**, 123 (1983).

¹⁴F. Ogata, T. Kambara, N. Sasaki, and K. I. Gondaira, *J. Phys. C* **16**, 1391 (1983).

¹⁵N. Sasaki and T. Kambara, *J. Phys. C* **15**, 1035 (1982).

¹⁶N. Sasaki and T. Kambara, *J. Phys. Soc. Jpn.* **56**, 3956 (1987).

¹⁷E. Meissner, H. Köppen, A. Spiering, and P. Gülich, *Chem. Phys. Lett.* **95**, 163 (1983).

¹⁸M. Mikami, M. Konno, and Y. Saito, *Chem. Phys. Lett.* **63**, 566 (1979).

¹⁹L. Wiehl, G. Kiel, C. P. Kohler, H. Spiering, and P. Gülich, *Inorg. Chem.* **25**, 1565 (1986).

²⁰Y. Tanabe and S. Sugano, *J. Phys. Soc. Jpn.* **9**, 766 (1954).

²¹E. König and K. J. Watson, *Chem. Phys. Lett.* **6**, 457 (1970).